# 3B Karaciğer Damar Segmentasyonu için MRF Tabanlı Birleşik Ölçek Seçimi ve Bölütlemesi Değerlendirmesi
# Assessment of MRF Based Joint Scale Selection and Segmentation for 3D Liver Vessel Segmentation Task

Neda B. Marvasti and Burak Acar
Department of Electrical and Electronics Engineering, BUSIM/VAVlab
Boğaziçi University
Istanbul, Turkey
Email: {neda.barzegarmarvasti, acarbu}@boun.edu.tr
URL: www.vavlab.ee.boun.edu.tr

***Özetçe* —Damar bölütlemesi medikal imge analizinde önemli bir yer tutmaktadır. Modaliteden bağımsız olarak, kullanılan bütün damar bölütleme yöntemlerinin ortak problemi damarlardaki ölçek, bir başka deyişle damar çapı, değişkenliğidir. Damar bölütlemesini ve ölçek belirlenmesini aynı anda çözmeye çalışan sınırlı sayıda girişime karşın, genel kabul gören yaklaşım analizin pekçok ölçekte yapılması ve sonuçların sonradan birleştirilmesidir. Yeni yayınlanan bir çalışmada, Hengameh et al. 2B retina görüntüleri için ölçek seçimi ve damar bölütlemeyi birlikte MRF kullanarak çözmeyi önermiştir. Bu çalışmada ise biz Hengameh et al. yöntemini 3B'a uyarlayarak, genel kabul gören, ve otomatik eşikleme ile imge rehberliğinde morfolojik firltreleme ile geliştirdiğimiz, çok ölçekli Hessian analizine dayalı yöntemle karşılaştıracağız. Karşılaştırma IRCAD verileri üzerinde nicel ve nitel olarak yapılmıştır. Sonuçlar MRF tabanlı algoritmanın, otomatik eşikleme ile imge rehberliğinde morfolojik filtreleme ile geliştirilmiş konvansiyonel algoritmaya göre belirgin bir üstünlüğünün olmadığını önermektedir.**

***Anahtar Kelimeler—Damar bölütleme; Damar segmentasyonu; Damar ölçek seçimi; Çok ölçekli konvansiyonel filtre; Min-Cut/Max-Flow; MRF Optimizasyonu; Imge rehberliginde morfolojik filtreleme.***

***Abstract*—Vessel segmentation plays an important role in medical image analysis. Irrespective of the modality used, the common challenge in all vessel tracking methods is scale variability, in other words, the dependence on the size of the vessels, which is unknown a priori. Despite few approaches that attempts to perform scale selection and segmentation simultaneously, the common approach is to perform multiscale analysis and fuse the results afterwards via a scale selection mechanism. Recently, Mirzaalian et al. proposed to use MRFs for joint scale selection and vessel segmentation in 2D retinal images. In this study, we have assessed the 3D version of this method in comparison with the conventional multiscale approach augmented with novel automatic threshold selection and image guided morphological filtering, using the well-known Hessian based method. The assessment has been done quantitatively using IRCAD dataset and qualitatively by studying the output vessel masks. The results indicate that the MRF based approach does not improve the results significantly in 3D liver vessel segmentation task compared to conventional multiscale approach.**

***Keywords—Vessel segmentation; Vessel scale selection; Conventional multiscale filter; Min-Cut/Max-Flow; MRF optimization; Image guided morphological filtering.***

## I. INTRODUCTION

Performing accurate and robust segmentation of vascular structures within the liver is an essential step in different medical applications, especially for surgical planning. The segmentation of vascular structures is challenging because of the variability in the vessel scales. Several specific methods have been proposed to segment vessels in contrast-enhanced liver CT images [1], [2], [3], [4]. Frangi et al. proposed a vesselness measure which is based on the geometrical analysis of the Hessian's eigensystem [5]. Hessian matrix at different scales is computed and simply the scale which gives the maximum vesselness response is chosen in every voxel. Manniesing et al. have enhanced the Frangi's method by combining it with a non-linear anisotropic diffusion scheme [6]. Although this algorithm gives more improved vessels, according to our practice, it requires more iterations which leads to high computation cost and time. Recently, Mirzaalian et al. have proposed the Markov random field (MRF) based optimization method to solve the scale-selection problem for 2D vessel segmentation [7].

In this paper, we assess the use of MRF scale selection in Hessian-based vesselness in the quality of vessel segmentation results compare to that of the the conventional multi-scale filter (CMF) method on 3D contrast enhanced CT liver images. We begin, in Section II, by reviewing the preliminaries of every

This work is in part supported by Boğaziçi University BAP (project number 5324) and TUBITAK CaReRa Project (project number 110E264).

978-1-4673-5563-6/13/$31.00 

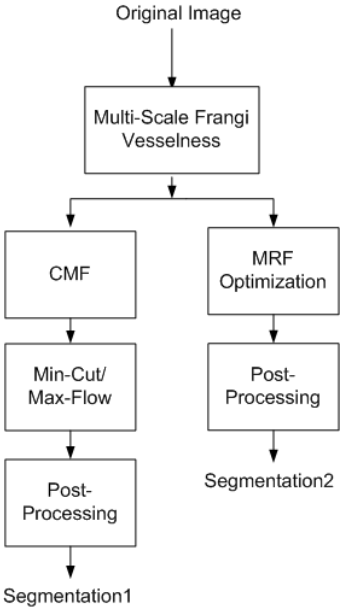


**Figure. 1:** Block diagram of the methods considered in the paper.

method that this paper focuses on. The proposed guided morphological dilation is presented in same section. In Section III, the experiments are evaluated and a CMF threshold selection method is proposed. Finally Section IV concludes the paper.

## II. Theory and Methods

The block diagram of two vessel segmentation methods, which are considered in this paper, are presented in Fig. 1. As shown in this figure, in the first method, we employ Min-Cut/Max-Flow algorithm after CMF to make the vessels thicker. The first step for both methods is multi-scale Frangi vesselness measure which computes the vesselness value in each voxel according to (1). The final step is post-processing which includes connected component analysis followed by a proposed image guided morphological filtering.

### A. Conventional Multi-scale Filter (CMF)

According to Frangi et al., vesselness function is defined as:

$$V_o(s) = \begin{cases} 0 & \lambda_2 > 0 \text{ or } \lambda_3 > 0, \\ (1 - exp(\frac{-R_A^2}{2\alpha^2}))exp(\frac{-R_B^2}{2\beta^2}))(1 - exp(\frac{-S^2}{2c^2})) & \text{o.w.}, \end{cases} \tag{1}$$

where $R_A$ is for distinguishing between plate-like and line-like structures, $R_B$ is for distinguishing blob-like structures, and $S$ measures the second order structureness. $\lambda_k$ is the $k^{th}$ eigenvalue of the Hessian matrix of the image, where $|\lambda_1| \leq |\lambda_2| \leq |\lambda_3|$. Definitions for $R_A$, $R_B$ and $S$ are given in (2).

$$R_A = \frac{|\lambda_2|}{|\lambda_3|}, R_B = \frac{|\lambda_1|}{\sqrt{|\lambda_2 \lambda_3|}}, S = \sqrt{\sum_{j \leq D} \lambda_j^2} \tag{2}$$

Therefor, after calculating $V_o$ at different scales (s), the maximum value of $V_o(s)$ at every voxel is set as the vesselness value at the same voxel and then, the vessel mask is created using a thresholding method.

### B. Min-Cut/Max-Flow Energy Minimization

According to Boykov et al., the given image is represented by the graph $g =< \nu, \xi >$, where nodes correspond to the voxels in the image and edges are links between them [8]. In our experiment, foreground hard constraint is calculated using vessel segmentation from CMF, i.e., a voxel is foreground if $vesselnessvalue > threshold$.
Background hard constraint is calculated from Hessian matrix of the image which is for the condition $|\lambda_1| \leq |\lambda_2| \leq |\lambda_3|$. A voxel is background if $(\lambda_2 \geq 0)$ or $(\lambda_3 \geq 0)$. $\lambda_k$ is the $k^{th}$ eigenvalue of the Hessian matrix of the image. For t-links we used vesselness image resulted from CMF which gives the vesselness value at every voxel and n-links are defined as

$$B_{p,q} \propto exp(\frac{-(I_p - I_q)^2}{2\sigma^2})(\frac{1}{dist(p,q)}). \tag{3}$$

### C. Scale-Selection using MRF Multi-Label Optimization

According to Mirzaalian et al. [7], we seek for labeling $f_p$ of each voxel $v_p$ that minimizes the following energy :

$$\begin{aligned} E(f) &= E_{data} + E_{boundary} \\ &= (1 - \mu) \sum_{p \in v} \varphi_p(f_p) + \mu \sum_{(p,q) \in \xi} \varphi_{pq}(f_p, f_q), \end{aligned} \tag{4}$$

where,

$$\begin{aligned} \varphi_p(f_p = s^i) &= (C_1) * (max_{s^j \in \{s^1, s^2, ..., s^k, s^{bg}\}} V(p, s^j) - V(p, s^i)) \\ \varphi_{pq}(f_p, f_q) &= (C_2) * min(1, |f_p - f_q|) \; ; (potts \; metric). \end{aligned} \tag{5}$$

$C_1$ is a constant to make V(.) integer, which is selected as $10^5$ in our experiment. $C_2$ is another constant to make the neighborhood term in the same range as data terms which is set to $C_2 = 10^3$.

Labels $s^1, s^2, ..., s^k$ are vesselness scales used in Frangi vesselness measure. The likelihood of choosing a vesselness label for a voxel is equal to that voxel's vesselness value at that label. A backgroundness label $s^{bg}$ is also introduced in this method and the backgroundness value is defined as:

$$v(x, s^{bg}) = \xi \; exp(\frac{-\overline{v}(x)}{\sigma^2}), \tag{6}$$

where, $\xi$ is the maximum vesselness value between all scales in all voxels. $\overline{v}(x)$ is the average vesselness value between all scales in the voxel $x$. In the result of this method, for every voxel a label is assigned which minimizes the energy $E(f)$.

### D. Post-Processing

Since there are some voxels presented as noise in the vessel mask, we first perform connected component analysis with a predefined threshold to remove small objects from the vessel mask. In this experiment this thresholdis set to 100. In the next step, an image guided morphological dilation with linear structures is carried out. In order to perform this task, 13 linear structures are defined in 13 directions with 45 degree in between. Then, the current vessel mask resulted from connected component analysis is dilated linearly in the direction of the vessels. For this purpose, the eigenvector related to $\lambda_1$ for the condition $|\lambda_1| \leq |\lambda_2| \leq |\lambda_3|$ at every voxel is calculated. $\lambda_k$ is the eigenvalue of the structure tensor

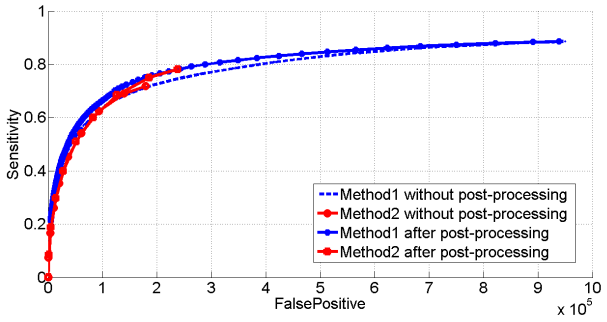


**Figure. 2:** The comparison between FROC curves of two segmentation methods before and after post-processing.

matrix of the CT image. After that, vessel mask is dilated for each voxel with a linear structuring element which is more aligned with the eigenvector derived at that voxel. As a result of this stage, we will have dilated voxels in the vessel direction.

## III. Experiments and Discussion

In this section, the performance and the accuracy of vessel segmentation results of scale selection methods, which have been reviewed in section II, are compared using FROC curves and visual criteria before and after post-processing steps. The algorithms are applied to 8 images selected from 3D contrast enhanced CT liver images of IRCAD database [1]. FROC curves are the average of FROC curve resulted from 8 experiments. ITK open source library is used for software programming and Matlab is used for plots. We used the liver mask given in this dataset as one of the inputs to the algorithms. In order to prepare the image for Frangi vesselness filter, the original image is cut according to a bonding box defined by user in order to decrease the computation time and values of the voxels lying outside of the liver mask are set to the average liver intensity value. Since the CT images are contrast enhanced, the vessels are seen as bright tubular structures within the liver. Frangi vesselness is calculated for 9 scales, linearly calculated between 1 and 5.

### A. Before Post-Processing

Fig. 2 shows the FROC curve of the segmentation results before any post-processing. In the first segmentation method (using CMF scale selection), FROC curve is calculated by changing the threshold of CMF method from 0 to 0.2 with interval of 0.001. For the second segmentation method (MRF based optimization scale selection), the FROC curve is calculated by changing the $\mu$ in (4) from 0 to 1 with interval of 0.1. For the sake of visual comparison, we select a proper threshold for CMF using Chi-squared histogram matching distance. To be able to do this, we initially cut the original image under the thresholded vessel mask, then we compare the histogram of every two sequential thresholds' histogram. Finally a threshold, in which we have the second maximum central difference between its previous and the next Chi-squared histogram distance, is chosen as an appropriate CMF threshold. According to the histogram distance shown in Fig. 3, maximum distance occurs in the threshold value of 0.02

[1] http://www.ircad.fr/softwares/3Dircadb/3Dircadb1/index.php?lng=en

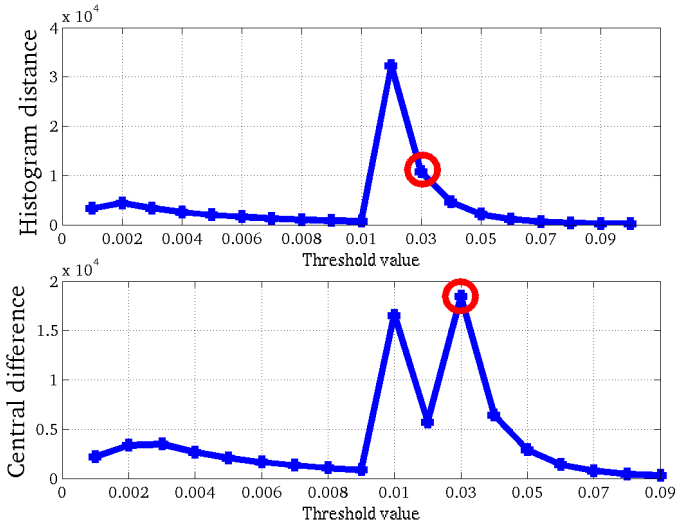


**Figure. 3:** The Chi-squared histogram distance and its corresponding central differences. In this experiment, the chosen threshold is 0.03.

which indicates that there is a large distance from threshold 0.02 to 0.03 because there are only vessels tissues in 0.03. This justifies the reason of choosing the second maximum in the central difference plot. Fig. 3 illustrates this procedure, where in this experience $threshold = 0.03$. For the parameter $\mu$ in MRF methos, we choose a $\mu$ which gives us the same amount of *False Positive* in FROC curves as the selected threshold value in CMF. In this experience, $\mu = 0.1$.
Fig. 4(a) through Fig. 4(d) show the visual segmentation results before post-processing. In this images, voxels which are in the ground truth but not in the vessel mask are shown in red (False-Negative), voxels which are in both ground truth and vessel mask are shown in green (True-Positive) and blue region shows voxels which are in the vessel mask but not in the ground truth (False-Positive).

### B. After Post-Processing

As described in section II.D, post-processing initially performs connected component analysis with threshold of 100 and then, it applies linear morphological dilation. Fig. 4(e) to Fig. 4(h) show the visual segmentation results after post-processing. In this images, as described above, voxels which are in the ground truth but not in the vessel mask are shown in red (False-Negative), voxels which are in both ground truth and vessel mask are shown in green (True-Positive) and blue region shows voxels which are in the vessel mask but not in the ground truth (False-Positive).

### C. Discussion

As shown in Fig. 2 and Fig. 4, although MRF based vessel scale selection algorithm gives high sensitivity in terms of FROC curves, visually we observe thicker vessels in medium size vessels which leads to including non-vessel voxels inside the vessel mask. Also small vessels are removed from the vessel mask. Moreover, MRF based method is very sensitive to the $\sigma$ value in (6) which requires to be chosen empirically. On the other hand, by performing Min-Cut/Max-Flow energy minimization on the results of segmentation via scale selection with CMF, we observe the same performance as MRF in terms

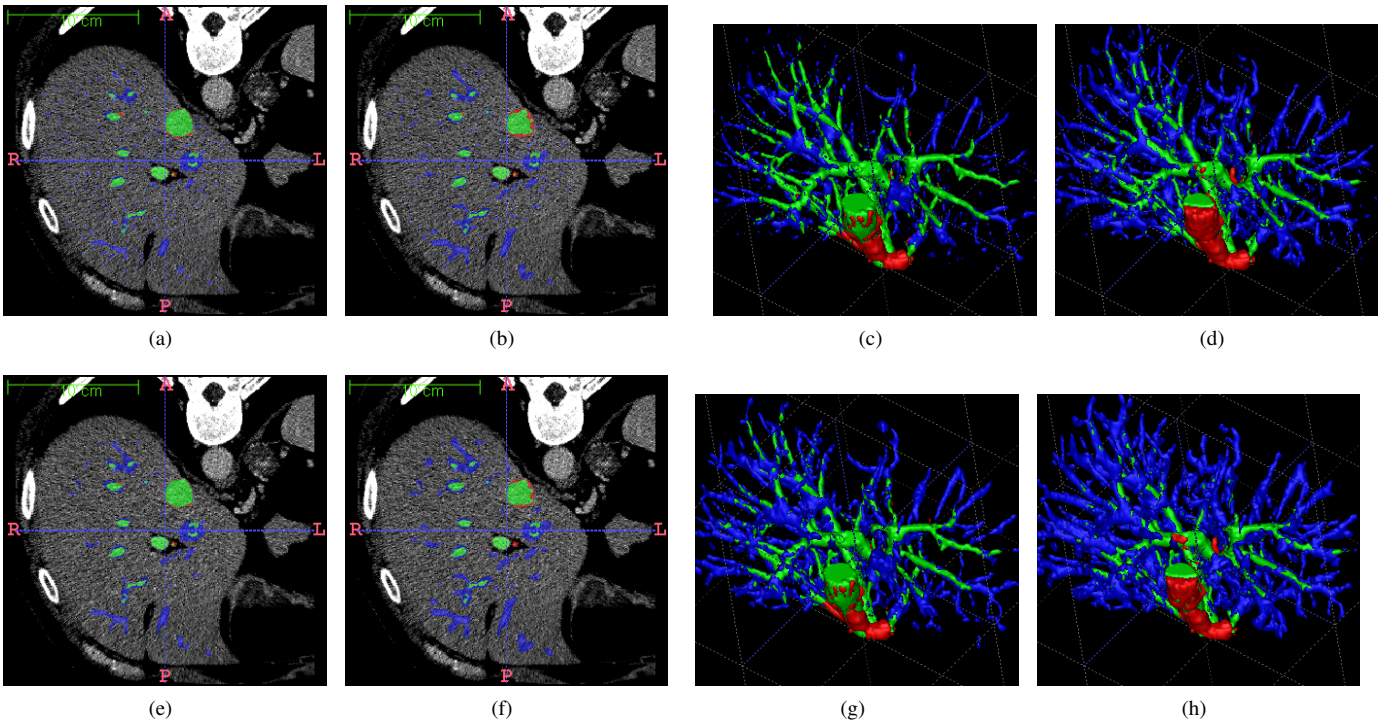


**Figure. 4:** Liver vessel segmentation results, the first and the second rows show vessel segmentation results before and after post-processing step, respectively. Plots (a,c,e and g) show 2D and 3D results of the first method (CMF + Min-Cut/Max-Flow) when $threshold = 0.03$ and (b,d,f and g) show 2D and 3D results for the second method (MRF based scale selection) when $\mu = 0.1$. Voxels which are in the ground truth but not in the vessel mask are shown in red. Voxels which are in both ground truth and vessel mask are in green. Voxels which are in the vessel mask but not in the ground truth are shown in blue.

of FROC curves. However, vessels are more like the ground truth in terms of thickness and thin vessels remain in the vessel mask. As illustrated in Fig. 2 and Fig. 4, using image guided morphological dilation results in improvement of FROC curve as well as visually connected vessel structures.
It is important to note that since we start with threshold 0 to calculate FROC curves of CMF, in smaller thresholds the whole image is covered as the vessel mask which results in high false positive. By increasing the threshold, false positive is decreased while sensitivity is still high.

## IV. Conclusion

Scale selection for multi-scale vessel segmentation methods is a controversial issue. A basic simple method to solve this problem is the use of CMF method which is basically selecting the maximum vesselness response at each voxel. Another approach is MRF based scale selection. In this paper, we assess the use of MRF scale selection in the Hessian-based vesselness maps as opposed to CMF method on 3D vessel segmentation. We compare the vessel segmentation results of these two methods in both visual and quantitative point of view. We further propose a post-processing approach which performs image guided linear dilation in the vessel directions. A threshold selection method for CMF is examined by utilizing the Chi-quadratic histogram distance. We show that by employing CMF method along with Min-Cut/Max-Flow energy minimization algorithm, more improvement in accuracy of the vessel segmentation is achieved compared to MRF scale optimization. In terms of computation time, both methods are fast, however CMF is faster than MRF-based one.

## References

[1] David Lesage, Elsa D. Angelini, Isabelle Bloch, and Gareth Funka-Lea, "A review of 3d vessel lumen segmentation techniques: Models, features and extraction schemes," *Medical Image Analysis*, vol. 13, no. 6, pp. 819 – 845, 2009, Includes Special Section on Computational Biomechanics for Medicine.

[2] Hua Li and A. Yezzi, "Vessels as 4-d curves: Global minimal 4-d paths to extract 3-d tubular surfaces and centerlines," *IEEE Transactions on Medical Imaging*, vol. 26, no. 9, pp. 1213 –1223, Sep. 2007.

[3] S. Esneault, C. Lafon, and J.-L. Dillenseger, "Liver vessels segmentation using a hybrid geometrical moments/graph cuts method," *IEEE Transactions on Biomedical Engineering*, vol. 57, no. 2, pp. 276 –283, Feb. 2010.

[4] Jens N. Kaftan, Hüseyin Tek, and Til Aach, "A two-stage approach for fully automatic segmentation of venous vascular structures in liver CT images," in *Medical Imaging 2009: Image Processing*, Orlando, USA, Feb. 2009, vol. 7259, pp. 725911–1–12, SPIE.

[5] Ro F. Frangi, Wiro J. Niessen, Koen L. Vincken, and Max A. Viergever, "Multiscale vessel enhancement filtering," 1998, pp. 130–137, Springer-Verlag.

[6] Rashindra Manniesing, Max A. Viergever, and Wiro J. Niessen, "Vessel enhancing diffusion: A scale space representation of vessel structures," *Medical Image Analysis*, vol. 10, no. 6, pp. 815 – 825, 2006.

[7] H. Mirzaalian and G. Hamarneh, "Vessel scale-selection using MRF optimization," in *IEEE Conference on Computer Vision and Pattern Recognition*, Jun. 2010, pp. 3273 –3279.

[8] Yuri Boykov and Gareth Funka-Lea, "Graph cuts and efficient n-d image segmentation," *Int. J. Comput. Vision*, vol. 70, no. 2, pp. 109–131, Nov 2006.